Cure-induced deformation of ultra-thin composite laminates

Federico Bosi*
University College London, London, WC1E 6BT, UK

Arthur Schlothauer†
ETH Zurich, 8092 Zurich, Switzerland

Sergio Pellegrino‡
California Institute of Technology, Pasadena, CA 91125, USA

In fiber reinforced composite materials, the manufacturing process induces residual stresses and distortions that decrease the mechanical performance of the structure and affect its geometry, especially in thin laminates. Multi-physics simulations were performed to assess the spring-in effect in ultra-thin composite parabolic solar reflectors. For this purpose, a resin kinetic model has been developed by means of differential scanning calorimetry experiments. The kinetic relation has been implemented into the finite element software in order to correctly predict the evolution of the composite degree of cure during the manufacturing process. Specimens were produced in an autoclave and their final geometries were measured by means of a non-contact measuring system and compared with numerical predictions, showing very good agreement.

I. Introduction

Fiber reinforced composite materials are widely used in aerospace lightweight structures because of their high ultimate strength per unit weight. Recent advancements in manufacturing of unidirectional carbon fiber prepreg materials have allowed the realization of ultra-thin unidirectional laminas by means of the tow-spreading technique. Ply-thickness on the order of 18-50 μm and an areal weight of 17 gsm is available, and laminates with a total thickness lower than 200 μm can be manufactured.[1] Thin cured composites are ideal in lightweight structures such as adaptive reflectors and mirrors,[2] as well as in aerospace systems where the bending compliance is a key factor for lower packaging volumes, such as deployable booms,[3] antennas and solar concentrators.

Many of these applications require very high shape accuracy of the final laminate, which is negatively affected by distortions that develop during long-term storage before launch and because of the manufacturing process. The former mechanism is a viscoelastic effect on the cured laminate that can be quantified through multi-scale simulations and experiments,[4,5] whereas the latter phenomenon takes place during curing of the composite and leads to structures whose final shapes differ from the mold geometries.[6] The main reason behind cure-induced distortion is the nonuniform distribution of residual stresses that develops during manufacturing processes and induces spring-in of curved parts, warpage of flat elements, and can ultimately lead to premature microbuckling, crack and delamination. Many mechanisms contribute to generating residual stresses during curing of fiber reinforced composite materials, which can be classified according to the scale at which they develop. Microscale residual stresses originate from the chemical shrinkage of thermoset resins during cross-linking and because of thermal anisotropy between fibers and resin. Macroscopic mechanisms

*Senior Lecturer, Department of Mechanical Engineering, Roberts building, Torrington Place. f.bosi@ucl.ac.uk

†Graduate Student, Department of Mechanical and Process Engineering, LEE building, Leonhardstrasse 21. arthursc@ethz.ch

‡Joyce and Kent Kresa Professor of Aeronautics and Professor of Civil Engineering, Graduate Aerospace Laboratories, 1200 E. California Blvd. AIAA Fellow. sergiop@caltech.edu

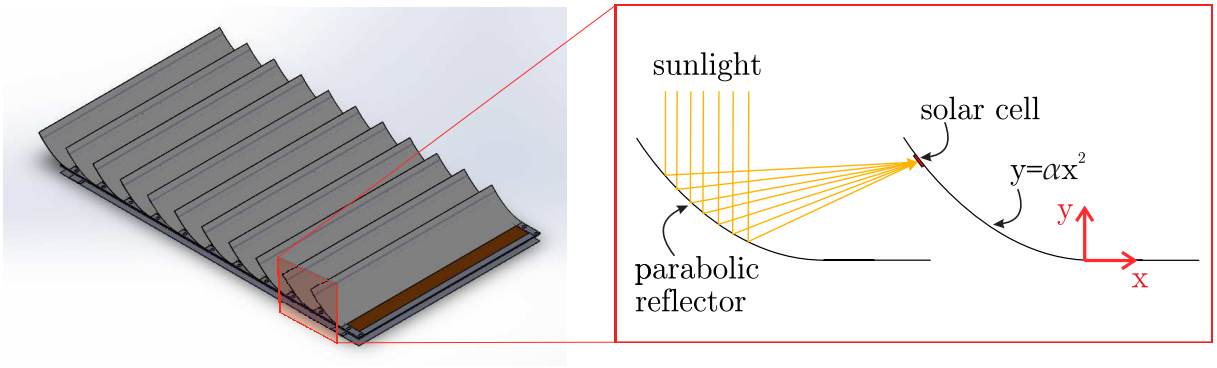

Figure 1. Left: Render of the tile structure for space solar power collection, containing an array of 11 parabolic composite reflectors. Right: schematic side view of the parabolic concentrator functionality. The correct shape will guarantee the sunlight reflection into the miniaturized solar cell positioned on the back of the previous reflector.

include the anisotropic response of individual plies, resin flow and compaction, and tool-part interaction. Therefore, the correct modeling of each aforementioned mechanism is fundamental for the prediction of final shape, property, fiber content and distribution of any composite structure. For this reason, many models have been developed to characterize curing of composites, ranging from the first simplified plane stress analysis through Classical Lamination Theory (CLT)[7] to more recent and complete three-dimensional thermochemical and viscoelastic simulations.[8]

The aim of the present study is to investigate for the first time the cure-induced residual stresses and deformations in ultra-thin laminates, while previous works were focused on composites with thicknesses greater than 1 mm.[9] Ultra-thin composites are more prone to deformation induced by the manufacturing process because of their lower stiffness, therefore the entire autoclave manufacturing process is simulated for a 144 μm thick parabolic solar concentrator, taking into account tool-part interaction and the thermo-kinetic process of the resin, which has been characterized in terms of degree of cure evolution during manufacturing. In order to reduce mass and increase the efficiency of satellites that collect solar power from space and transmit it to receiving stations on Earth, lightweight parabolic composite reflectors have to focus the reflected sunlight onto miniaturized photovoltaic cells, Fig. 1. In the present work, the concentrators are uncoated, while their final configuration presents a reflective coating. The shape of the reflector can be described through the equation $y = \alpha x^2$ (x is in mm), where the quadratic coefficient of the parabola α has to be equal to 0.033 mm^{-1} in order to meet design requirements.

Therefore, the modeling of the manufacturing-induced distortion and the correct prediction of the composite final geometry is fundamental to achieve high shape efficiency, which is defined as the ratio between the power incident on the solar cell and the power arriving at the reflector. Experiments, Sect. II, and multi-physics simulations, Sect. III, were performed in order to quantify the change from the nominal parabolic mold shape in ultra-thin composite solar reflectors, Sect. IV.

II. Manufacturing of ultra-thin solar concentrators

The composite material used for the manufacturing of solar reflectors consists of a 17 gsm (fiber areal weight) unidirectional prepreg made of Toray T800H fibers embedded in a ThinPreg™ 120EPHTg-1 epoxy matrix, supplied by North Thin Ply Technologies (NTPT). Each ply has a nominal cured thickness of 18 μm and 60% of fiber volume fraction. The symmetric composite layup consists of 8-ply laminate with a $[90/0/+45/\text{-}45]_S$ stacking orientation (0° along the parabola arc-length), with a total thickness of 144 μm. A rectangular 100 mm × 25 mm layup was placed on top of a parabolic rigid steel mold (topped with a release agent), whose parabolic coefficient is α =0.025 mm^{-1}. This value has been chosen to try to compensate the spring-in effect and obtain a final composite shape closer to the geometrical requirement (α =0.033 mm^{-1}). Layers of Peel-Ply, breather, and vacuum foils were placed onto the composite layup. The manufacturing process is reported in Fig. 2.

Three different samples were cured in an autoclave following the cure specified by NTPT. The temperature

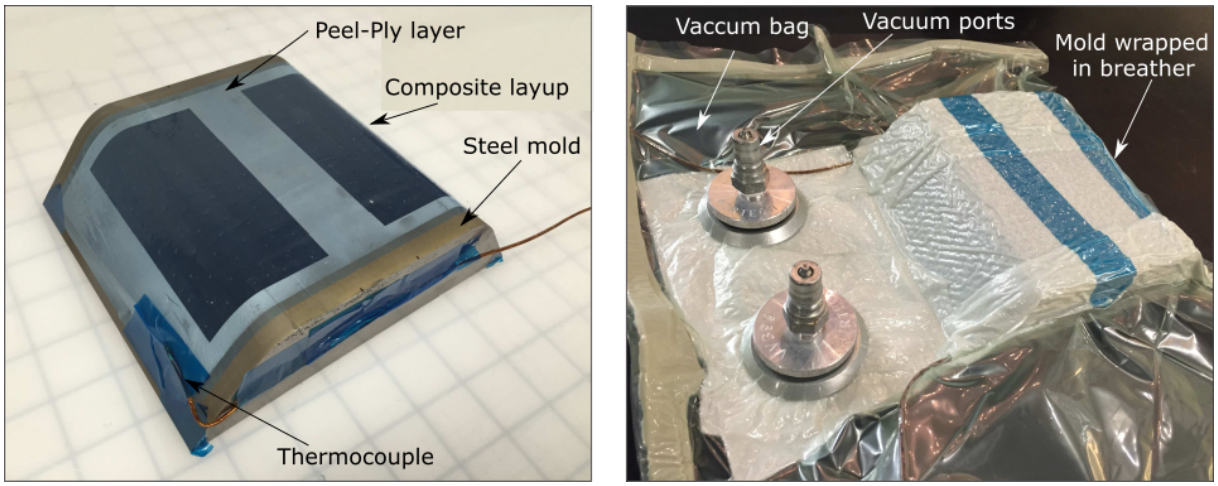

Figure 2. Manufacturing process of two parabolic reflectors on a steel mold.

was increased at a rate of 2°C/min from 20°C to 80°C, kept constant for 30 min and increased at the same rate until 120°C. This curing temperature was maintained for 2 hours, before the final cooling phase at -2°C/min was performed. A pressure of 80 psi was applied during the entire process.

The manufactured reflectors were measured by means of FaroArm (Faro®) non-contact laser measurement system, Fig. 3. A parabolic least-squares fit was applied for each section along the reflector width in order to evaluate the change in the quadratic coefficient α of the parabola with respect to the nominal shape of the mold. Results of the three experiments, reported in Fig. 4, show that the parabolic coefficient α varies between 0.028 mm^{-1} and 0.0295 mm^{-1}, and it remains almost constant along the width of the reflector. As expected, the laminate is subjected to spring-in effect, which increases the parabolic coefficient by 14% on average. However, the final shape of the composite does not match the requirement of α =0.033 mm^{-1}. Therefore, the mold shape has to be changed in order to obtain the final part of the desired geometry. Numerical simulations of the process-induced deformation will allow a fast optimal design of the mold, avoiding an expensive and time-consuming iterative approach to trying different mold configurations.

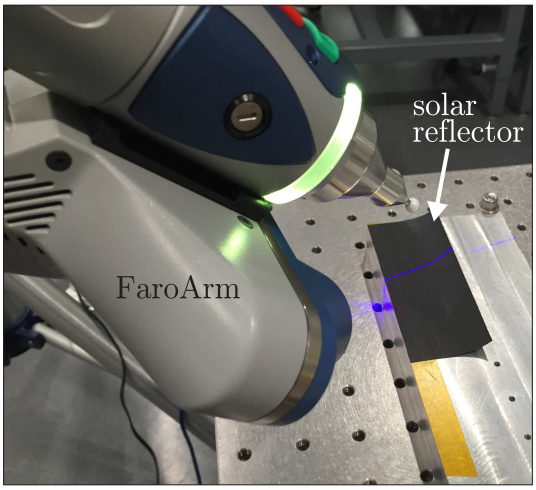

Figure 3. Experimental setup for the measurement of the final shape of the cured composite concentrator using the FaroArm laser measurement system.

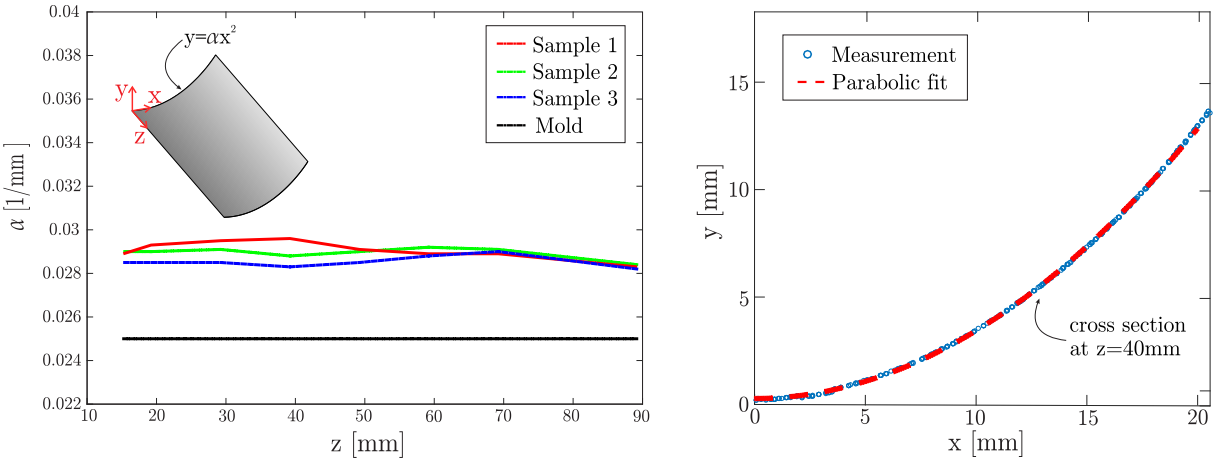

Figure 4. Left: variation of the quadratic parabolic coefficient α of the 8-ply reflector along its width. Right: the parabolic fit on a composite cross section at $z = 40$ mm. The shape of the reflector after cure can be very well described by a parabolic curve.

III. Multi-physics modeling of the curing process

The correct characterization of the evolving properties of the fiber reinforced material during the manufacturing process requires a multi-physics simulation where heat transfer, chemical reaction, flow and compaction processes are simultaneously considered. For this purpose, the COMPRO Complete Component Architecture CCA (Convergent Solution) plug-in to Abaqus/Standard finite element solver (R2016x, Dassault Systemes) was used. COMPRO is a multi-physics code designed to account for all major sources of manufacturing-induced residual stresses and deformations. It is based on the integrated sub-model approach[10] and it consists of the thermo-chemical, flow-compaction and stress-deformation modules. The thermochemical module is divided into two submodules which analyze the heat transfer and the resin cure kinetic. Although the two submodules governing equations are coupled because the resin generates heat during cross-linking reaction, they are solved independently by means of an iterative Euler implicit scheme. The outputs of this module are the temperature profile throughout the tool and composite parts, as well as the degree of cure of the laminate which affects the evolution of resin flow and elastic properties in the subsequent modules. For this reason a resin kinetic model was developed and is reported in the following subsection. Furthermore, the COMPRO flow-compaction module calculates the evolution of viscosity, volumetric and unidirectional cure shrinkage. Finally, the stress-deformation module analyzes the variation of residual stresses and deformations during the autoclave cure cycle. The evolution of the composite elastic constants is obtained through a micro-mechanical approach[11] considering a cure hardening instantaneously linear elastic constitutive relation (CHILE).

A. Resin cure kinetic characterization

Accurate material models are fundamental in order to obtain faithful results from numerical simulations, especially when a material undergoes changes of thermo-mechanical and chemical properties. It is well known that thermoset resins employed in fiber-reinforced composites cure as the effect of an exothermic cross-linking reaction triggered by a thermal loading condition.

The resin employed in the prepreg is a toughened epoxy (ThinPreg™402 from NTPT) developed for an autoclave molding process with a recommended standard cure cycle at 120°C for 2 hours, Sect. II. Since in the COMPRO material database there is no resin that fully cures at 120°C and has similar properties to the one used in this study, a characterization of the resin cure kinetic was performed.

In order to develop a kinetic model, Differential Scanning Calorimetry (DSC) tests[12] were carried out on 7-10 mg of neat resin, using a Perkin Elmer DSC-7, Fig. 5 (left). The resin was encapsulated in a standard aluminum hermetic pan, and the weight w was measured before and after the test with a Mettler Toledo AE 240 analytical balance, without showing any mass losses during the DSC tests. The Differential Scanning

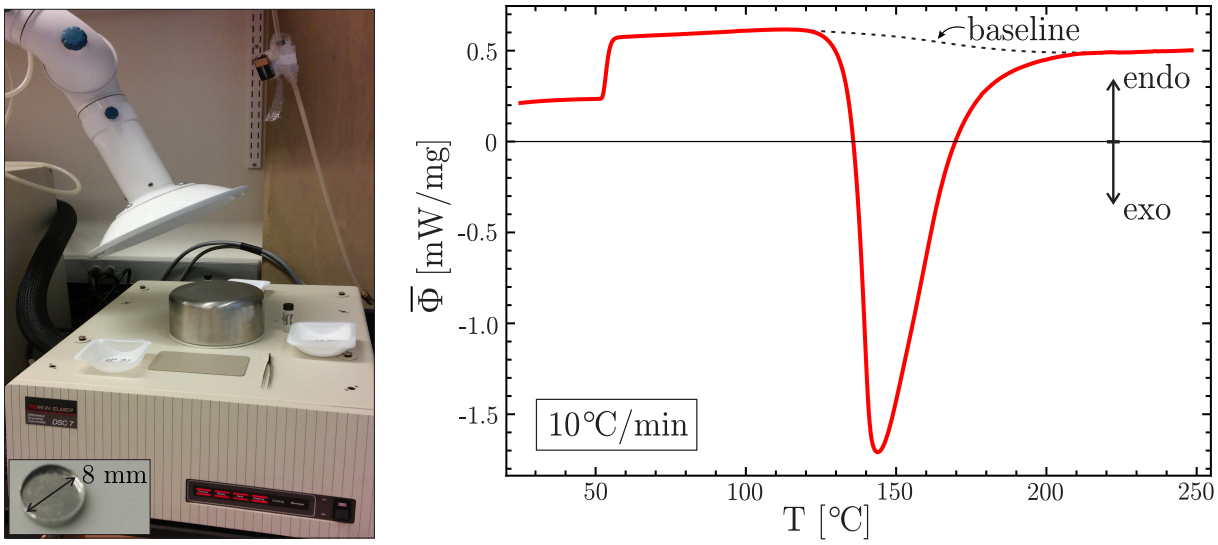

Figure 5. Left: Differential Scanning Calorimeter (DSC) employed in the resin cure kinetic modeling; the aluminum hermetic DSC pan containing 7-10 mg of resin is shown in the inset. Right: specific heat flow $\bar{\Phi} = \Phi/w$ as a function of temperature during a DSC dynamic thermal scan performed at 10°C/min for an uncured sample. The glass transition temperature is at 53.09°C, while the exothermic peak occurs at 143.37°C. The dashed black line represents the baseline, necessary to calculate the amount of heat generated during cross-linking.

Calorimetry measures the heat flow Φ generated by the material during the test, from which the enthalpy of the reaction H can be obtained as the area enclosed by the exothermic heat flow curve $\Phi(\tau)$ and the baseline:

$$H(t) = \int_{t_0}^{t} \Phi(\tau) \mathrm{d}\tau, \tag{1}$$

where t_0 is the time at which the reaction begins. Therefore, the time evolution of the resin degree of cure x is defined as[13]

$$x(t) = \frac{H(t)}{H_T}, \tag{2}$$

where H_T is the total heat of the reaction. The degree of cure x varies between 0 and 1, where $x = 0$ represents the uncured material, while $x = 1$ is the fully cured resin.

In the present study, the variation of the degree of cure as a function of the temperature and time has been assessed through isothermal measurements. Three isothermal cure temperatures (T=[100, 120, 135]°C) were chosen between the onset of the reaction and the peak heat flow from a dynamic temperature scan on uncured resin performed at 10°C/min. The DSC cell was rapidly heated to the desired cure temperature, which was held constant for 15, 30, 60 and 120 minutes. At the end of each isothermal test, a dynamic scan was performed, where the temperature was raised from 25°C to 250°C at a rate of 10°C/min in order to measure the residual heat of the reaction H_R. For isothermal measurements, the degree of cure is defined as

$$x = \frac{\bar{H}_T - \bar{H}_R}{\bar{H}_T}, \tag{3}$$

where $\bar{H}_T = 342.37$ J/g is the total specific enthalpy of reaction measured at 10°C/min on the uncured resin. The values of the specific residual heat of the reaction $\bar{H}_R$ for the performed tests are reported in Table 1. The result of one dynamic DSC scan on uncured resin is shown in Fig. 5 (right). In the same plot, the glass transition temperature can be obtained from the inflection point of the step-wise transition.

The analytical kinetic model is assumed to obey the phenomenological relation developed for an autocatalytic reaction modified to account for diffusion.[14] This model has the advantage to be already implemented into COMPRO and used to describe the behavior of other resins. The rate of reaction $\mathrm{d}x/\mathrm{d}t$ can be written as

Table 1. Specific residual heat of the reaction $\bar{H}_R$ [J/g] for isothermal DSC tests

time [min]	100°C	120°C	135°C
15	329.65	65.06	13.02
30	233.44	26.27	3.29
60	124.90	17.45	1.58
120	73.50	6.03	0.20

$$\frac{\mathrm{d}x}{\mathrm{d}t} = \frac{Kx^m(1-x)^n}{1+e^{C(x-x_{C0}-x_{CT}T)}}, \tag{4}$$

where m and n are exponential constants, C refers to the diffusion constant, x_{C0} is the critical degree of cure at $T = 0$K, while x_{CT} is a constant relating the critical resin degree of cure and the temperature. K is defined through an Arrhenius expression

$$K = Ae^{-\Delta E/RT}, \tag{5}$$

where A is the pre-exponential factor, ΔE is the activation energy, and R=8.314 J/(mol K) is the universal gas constant.

The model parameters were obtained by fitting the results from the DSC isothermal tests and are reported in Table 2. The developed mathematical model was used to predict the evolution of the resin degree of cure x during isothermal tests at 100°C, 120°C and 135°C. The results of theoretical predictions are compared with the experimental measures in Fig. 6, showing a good agreement.

Table 2. Kinetic model parameters

A [1/s]	ΔE [J/mol]	m	n	C	x_{C0}	x_{CT} [1/K]
$4.53 \cdot 10^6$	$6.65 \cdot 10^6$	0.803	0.606	6.59	-1.65	$5.48 \cdot 10^{-3}$

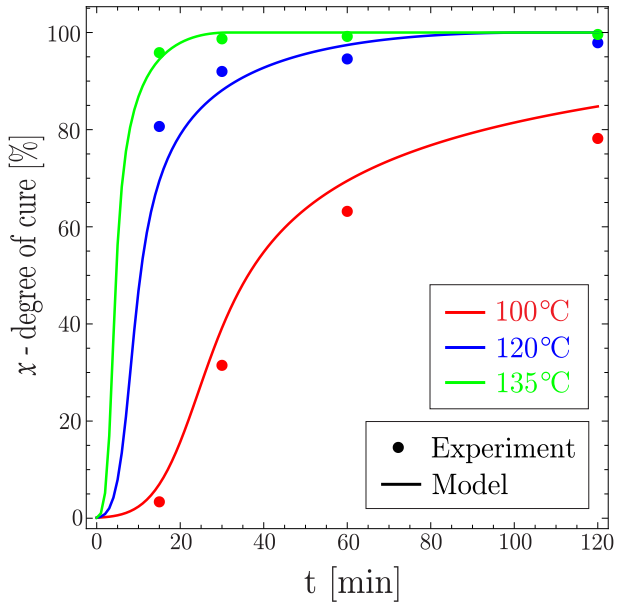

Figure 6. Kinetic model through isothermal DSC tests: comparison between theoretical predictions and measurements from experiments performed at 100°C, 120°C and 135°C for 15,30,60, and 120 minutes.

B. Finite element simulation

A parabolic solar reflector section was investigated to assess the process induced deformation. The symmetric composite layup reproduces the experimental setup and consists of 8-ply laminate with a $[90/0/+45/\text{-}45]_s$ stacking orientation (0° along the parabola arc length), and a total thickness of 144 μm. In order to reduce the computational time, only one cross-section of the reflector width was considered. The parabolic composite and tool geometries match the experiments, with a laminate arc length of 25 mm. In order to correctly capture through-thickness effects, it is desirable to employ quadratic 20 nodes solid elements. However, due to the extremely small thickness of the studied laminate, linear elements give the same results as quadratic elements (0.67 % difference), therefore DC3D8 elements were employed in the thermo-chemical analysis, while C3D8 were adopted for the stress-deformation module. The composite laminate and the steel mold were modeled in Abaqus R2016X with 4592 and 17220 elements, respectively. An example of the mesh is reported in the inset of Fig. 7, where it can be observed that one solid element per ply thickness was used in order to achieve enough through-thickness resolution.

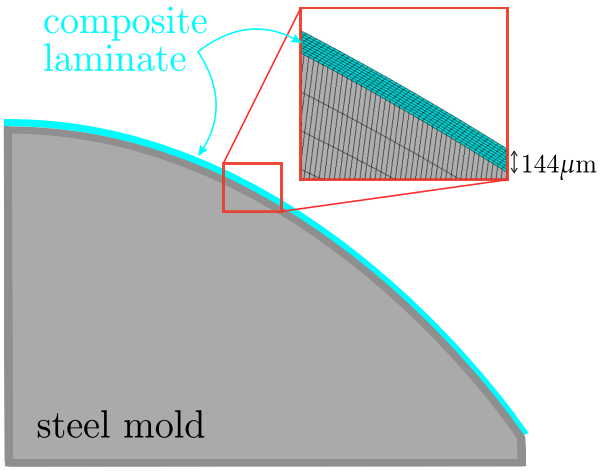

Figure 7. Composite laminate and tool assembly for a parabolic reflector modeled in Abaqus R2016X finite element software.

A user-defined material was created in COMPRO in order to describe the behavior of the NTPT prepreg used, Sect. II. The composite thermo-chemical properties were implemented following the model developed in Sect. A for the resin. The variation of the resin elastic constants and rheology during the cure cycle, required in the stress-deformation and flow-compaction analyses, should be experimentally determined through DMA, TMA or rheometer experiments, and implemented in the finite element software once their mathematical models are developed. In absence of those properties, the flow-compaction module was not considered, while the resin mechanical properties were assumed to follow the behavior of the fully characterized Hexcel 8552 resin, available in the material database. The resin properties were defined such that the elastic constants of the fully cured composite ($x = 1$) match the experimental values measured for the same material.[15] The elastic properties of the Toray T800H fibers were available in the material database, so that the constants of the composite materials were autonomously calculated by COMPRO plug-in through the implemented micro-mechanical approach.

A discrete coordinate system was defined for the laminate, with the 1-direction along the 0° of ply orientation and the 3-direction through the thickness. The temperature and pressure profiles described in Sect. II were implemented in the simulation. The convective heat transfer was assumed only on the top surface of the laminate and lateral surfaces of the mold, with a heat transfer coefficient equal to 80 W/m^{2}K.

The results of the thermochemical analysis are reported in Fig. 8, showing the time evolution of the temperature and the degree of cure in the composite part.

The outputs of the thermochemical module were used as inputs for the stress-deformation analysis, where a surface to surface contact was defined to model the tool part interaction. Hard normal contact and a tangential friction coefficient of 0.15 were employed to define contact properties. A final tool-removal step was set up to evaluate the spring-in effect. During this step, the steel mold was removed and the

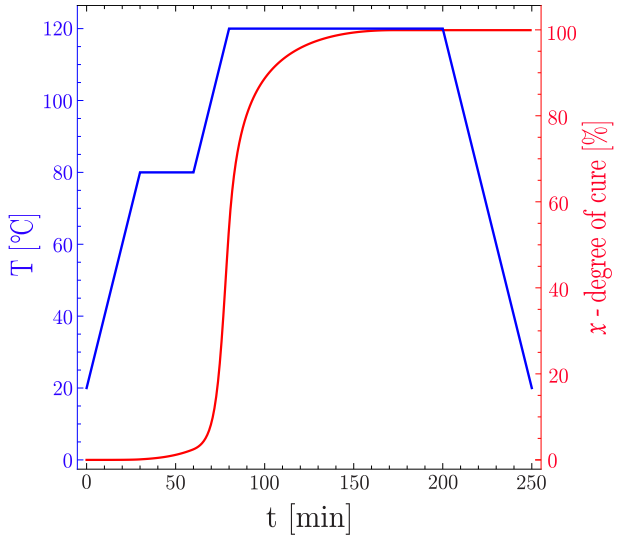

Figure 8. Temperature and degree of cure profiles in the composite laminate during the manufacturing process.

boundary conditions on the composite laminate were changed in order to allow the sample to deform (only the displacements of the bottom-left corner of the laminate were constrained, allowing rotation of the reflector).

IV. Results and discussion

Results of the numerical simulations are reported in Fig. 9, where the initial shape of the laminate (due to the mold geometry) and its deformed configuration at the end of the curing process after the tool removal are shown. The spring-in effect is evident and strongly affects the final shape of the solar reflector.

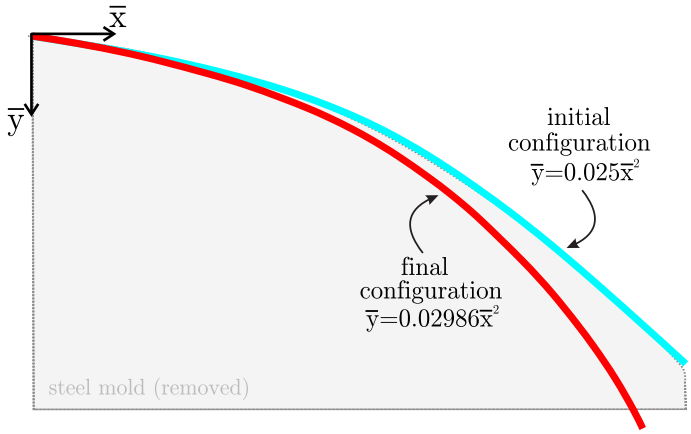

Figure 9. Spring-in effect for the composite parabolic reflector obtained through finite element simulations: undeformed and deformed (at the end of the manufacturing process, after the tool removal step) configurations are reported in light blue and red, respectively.

The process-induced deformation was quantified by measuring the change in the quadratic coefficient α of the parabolic shape of the reflector. The coordinates of the elements at the inner edge of the laminate were extracted from the result of the numerical simulation and imported into Mathematica v.11.0 (Wolfram Research). A least-square fit (FindFit function in Mathematica) was employed to calculate the parabolic coefficient of the deformed part, $\alpha = 0.02986$ mm^{-1} (the standard error in the parabolic coefficient fit was 0.23). The predicted value of the parabolic coefficient is reported in Fig. 10 together with its measurements from the three experiments performed. It can be noted that the numerical simulation of the cure-induced

deformation is able to correctly capture the variation in the shape of the composite reflector, with a 6.24% maximum error between finite element prediction and experimental results.

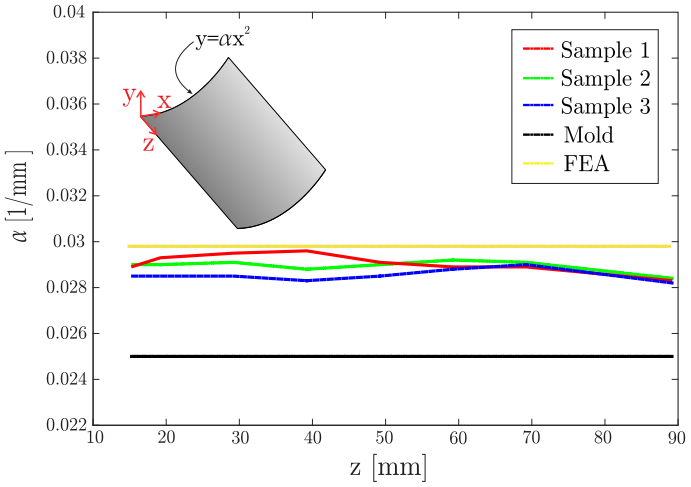

Figure 10. Variation of the quadratic parabolic coefficient α of the 8-ply reflector along its width: experimental measurements of three samples (red, blue and green lines) are reported together numerical prediction (yellow line) and mold shape (black line).

Although the result of the finite element analysis matches well the experimental measurements, numerical simulations will be further improved by fully characterizing the constituent resin in terms of viscosity, permeability, variation of (visco)elastic material parameters and coefficients of thermal expansion. The development of a full material model will contribute to obtaining accurate results that will enhance the performance of the resulting structural composite solar reflectors. Once the material behavior is correctly modeled, the influence of several parameters on the spring-in effect can be studied, including cure pressure, resin flow-compaction, mold materials, friction coefficients, and the presence of a release layer between the tool and composite parts. Finally, the existence of a flat part at one edge of the parabolic reflector, neglected in this study, should be investigated as a potential source of a larger spring-in effect.

V. Conclusion

The deformation induced by the manufacturing process of thin composites affects their final shape, potentially compromising the structural and geometry requirements. Therefore, the spring-in effect of an ultra-thin parabolic solar reflector manufactured with fiber reinforced material has been experimentally and numerically investigated.

A customized steel mold was realized for the manufacturing of an 8-ply laminate made with a lightweight 17 gsm unidirectional prepreg, while a non-contact laser measuring technique was employed in the measurement of the final shape of the composite element after the autoclave cure cycle. Furthermore, the variation of the material thermo-chemical properties during cure was assessed by developing a resin kinetic model through isothermal differential scanning calorimetry experiments. Lastly, numerical simulations were performed in order to replicate the process-induced deformation of the parabolic reflector. Variations of the composite thermo-chemical and mechanical properties during cure were considered, and they are fundamental in order to accurately predict the experimental change of the laminate shape.

The developed numerical procedure will help the mold shape optimization by accounting for the cure-induced spring-in effect, and it can be potentially extended to any composite structure. Therefore, the accurate determination of the process-induced deformations will allow a faster and more accurate manufacturing process of composite structures.

Acknowledgments

Financial support from the Northrop Grumman Corporation is gratefully acknowledged. DSC experiments were performed in the Kornfield Lab at the California Institute of Technology: we thank Dr. T. Di Luccio and Mr. K. Ramachandran for helpful comments and discussions. The manufacturing and measurements of composite laminates were carried out at the Space Structure Laboratory at the California Institute of Technology. Numerical simulations were performed using COMPRO simulation software package for Abaqus, developed by Convergent Manufacturing Technologies.

References

[1]Amacher, R., Cugnoni, J., Botsis, J., Sorensen, L., Smith, W., and Dransfeld, C. *Thin ply composites: Experimental characterization and modeling of size-effects*, Composites Science and Technology, 110, 121132 (2014).

[2]Steeve, J. and Pellegrino, S. *Ultra-thin highly deformable composite mirrors*, 54th AIAA Structures, Structural Dynamics, and Materials Conference (2013).

[3]Leclerc, C., Wilson, L., Bessa, M., and Pellegrino, S. *Characterization of ultra-thin composite triangular rollable and collapsible booms*, 4th AIAA Spacecraft Structures Conference, AIAA SciTech Forum (2017).

[4]Brinkmeyer, A., Pellegrino, S. and Weaver, P.M. *Effects of long-term stowage on the deployment of bistable tape springs*, Journal of Applied Mechanics 83 (1), 011008 (2016).

[5]Kwok, K. and Pellegrino, S. *Micromechanics models for plain-weave composite tape springs*, AIAA Journal, 55 (1), 309-321 (2017).

[6]Baran, I., Cinar, K., Ersoy, N., Akkerman, R., and Hattel, J.H. *A Review on the Mechanical Modeling of Composite Manufacturing Processes*, Archives of Computational Methods in Engineering 24 (2), 365-395 (2017).

[7]White, S.R., and Hahn, H.T. *Process modelling of composite materials: residual stress development during cure. Part II. Experimental validation*, Journal of Composite Materials 26 (16), 2423-2453 (1992).

[8]Zhu, Q., Geubelle, P.H., Li, M., and Tucker, C.L. *Dimensional accuracy of thermoset composites: simulation of process-induced residual stresses*, Journal of Composite Materials, 35 (24), 2171-2205 (2001).

[9]Cinar, K., Oztrk, U.E., Ersoy, N., and Wisnom, M.R. *Modelling manufacturing deformations in corner sections made of composite materials*, Journal of Composite Materials, 48 (7),799-813 (2014).

[10]Loss, A.C., Springer, G.S. *Curing of epoxy matrix composites*, Journal of Composite Materials, 17, 135-169 (1983).

[11]Bogetti, T.A., Gillespie, J.W. *Process-Induced Stress and Deformation in Thick-Section Thermoset Composite Laminates*, Journal of Composite Materials, 26 (5), 626-660 (1992).

[12]Rosu, D., Cascaval, C.N., Mustata, F., Ciobanu, C. *Cure kinetics of epoxy resins studied by non-isothermal DSC data*, Thermochimica Acta, 383, 119-127 (2002).

[13]Hardis, R., Jessop , J.L.P., Peters, F.E., Kessler , M.R. *Cure kinetics characterization and monitoring of an epoxy resin using DSC, Raman spectroscopy, and DEA*, Composite Part A, 49, 100-108 (2013).

[14]Hubert, P., Johnston, A., Poursartip, A., Nelson, K. *Cure kinetics and viscosity models for Hexcel 8552 epoxy resin*, 46th International SAMPE Symposium and Exhibition, 2341-2354 (2001).

[15]Steeves, J., Pellegrino, S. *Post-cure shape errors of ultra-thin symmetric CFRP laminates: effect of ply-level imperfections*. Composite Structures, 167, 237-247 (2017).